



HAL
open science

Experimental Analysis of Capacity Degradation in Lithium-ion Battery Cells with Different Rest Times

Brian Ospina Agudelo, Alessandro Massi Pavan, Walter Zamboni, Rebecca Todd, Andrew Forsyth, Eric Monmasson, Giovanni Spagnuolo

► To cite this version:

Brian Ospina Agudelo, Alessandro Massi Pavan, Walter Zamboni, Rebecca Todd, Andrew Forsyth, et al.. Experimental Analysis of Capacity Degradation in Lithium-ion Battery Cells with Different Rest Times. 2020 2nd IEEE International Conference on Industrial Electronics for Sustainable Energy Systems (IESES), Sep 2020, Cagliari, Italy. pp.44-49, 10.1109/IESES45645.2020.9210657 . hal-03271392

HAL Id: hal-03271392

<https://hal.science/hal-03271392>

Submitted on 16 Mar 2024

HAL is a multi-disciplinary open access archive for the deposit and dissemination of scientific research documents, whether they are published or not. The documents may come from teaching and research institutions in France or abroad, or from public or private research centers.

L'archive ouverte pluridisciplinaire **HAL**, est destinée au dépôt et à la diffusion de documents scientifiques de niveau recherche, publiés ou non, émanant des établissements d'enseignement et de recherche français ou étrangers, des laboratoires publics ou privés.

Copyright

Experimental analysis of capacity degradation in lithium-ion battery cells with different rest times

Brian Ospina Agudelo^{*†}, Alessandro Massi Pavan[‡], Walter Zamboni^{*},
Rebecca Todd[§], Eric Monmasson[†] and Giovanni Spagnuolo^{*}

^{*} DIEM - Università degli studi di Salerno, Via Giovanni Paolo II, 132 - 84084 Fisciano (SA), Italy

[†] Laboratoire SATIE - Université de Cergy-Pontoise,

SATIE 5 Mail Gay-Lussac - Neuville-sur-Oise 95031 Cergy-Pontoise

[‡] DIA - Università degli studi di Trieste, Via Alfonso Valerio 6/1, 34127 Trieste (TS), Italy

[§] Department of Electrical & Electronic Engineering - The University of Manchester,

Oxford Road, Manchester M13 9PL, United Kingdom

e-mail: bospinaagudelo@unisa.it

Abstract—This work presents the comparison of the variations in the electrical performance of two lithium-ion batteries during a cycling experiment. The experiment consists in a sequence of full charge/full discharge cycles, with constant current and constant voltage phases for the charge and the discharge. The main difference between the tests conducted over the two batteries is the rest time after charge in each cycle. For one battery, this time is one hour, while for the other one is one minute. The analysis was performed in terms of capacity, charge-discharge times, voltage evolution during the rest period and internal resistance. The results show that, in terms of the characteristics analyzed, there is not a considerable difference in the degradation behavior of the two batteries, which may mainly be due to the relatively-short length of the rest periods with respect the time constants related to phenomena, such as the capacity recovery.

Index Terms—battery aging, cycling test, internal resistance, rest time, efficiency, voltage relaxation.

I. INTRODUCTION

The growing demand for sustainable solutions in the fields of electricity generation, as is the case of photovoltaic and wind based power systems, and transportation, more specifically electric and hybrid vehicles, has accentuated the need for reliable energy storage devices. Mainly, due to the compromise between power and energy density and other characteristics such as relative long life and environmental friendliness, lithium-ion batteries are particularly well suited for alternative power generation and transportation applications [1].

The capability of batteries for storing and delivering energy reduces over time. Battery performance is not only degraded during use, namely charge-discharge cycling under specific operation conditions [2], but also during rest periods [3]. Normally, this degradation processes are manifested as reductions in the battery capacity or increases in its equivalent impedance for given operation conditions [4]. The characterization of the variation of battery specific performance parameters with aging is required in tasks such as estimation procedures correction, failure detection and degradation mechanisms modeling.

This work is supported in part by University of Salerno FARB funds and PhD program funds. This work is also supported by a public grant overseen by the French National Research Agency (ANR) as part of the “Investissements d’Avenir” program (reference: ANR-16-IDEX-0008)

The degradation of batteries is generally evaluated making use of calendar or cycling tests, whose results can be used to establish models for the battery parameters degradation based on empirical laws.

A cycling aging test is normally performed by applying a charge-discharge profile, which may be based on a particular experimental battery use regime, periodic [2], [5]–[7] or even randomly generated, under specific operation conditions during a given period of time. During this test time additional tests, such as capacity reference cycling or electrochemical impedance spectroscopy [2], [6], can be performed at different points in order to extract information that can be used for battery response and aging characterization or modeling. The effects of calendar aging can be studied by storing a battery under specific conditions [8], [9], mainly temperature and State of Charge (SOC), and performing characterization tests periodically. For a complete evaluation of the degradation mechanism in a battery, both kinds of aging tests can be alternated [10], [11].

The data derived from cycling tests can be used for proposing degradation models [8], [10], mainly for the capacity [7], [9], [12] and the equivalent series resistance. The results of aging testing can also be useful for characterizing the variations of battery models parameters with aging, including equivalent circuit, impedance [2] and electrochemical models. Furthermore, the effects of specific characteristics of the cycling profiles on the batteries degradation can also be analyzed. For instance, there are studies focused on the charge or discharge rate values, the range of SOC covered, the dynamic characteristics of the profile, and the effects of the inclusion of rest periods at different points of the cycle [5], [6], [13].

The effect of the length of the rest periods included in the charge-discharge profile has been previously studied in works such as the ones presented on [5], [6], [10]. In [10], the capacity recovery phenomenon was studied when a rest period is periodically included after a fixed amount of days. Something similar was done in [5], but adding rest periods after a fixed number of cycles. It is worth mentioning that in both [5] and [10] the rest periods are of the order of days. In this studies,

higher overall degradation rates were observed when the rest periods were not included in the cycling tests. This is mainly due to the increases in capacity and the reductions in the series resistance observed during the rest periods. Shorter rest periods were considered in the experiments performed in [6], included after a fixed number of continuous cycles and also in each cycle between the charge and discharge sections. The results pointed out that significant variations in the capacity degradation rate can only be appreciated after rests periods higher than two hours applied periodically after a fixed amount of cycles. Moreover, it was concluded that the effect of a long rest in the cycling introduced after multiple full cycles has a positive effect over the capacity degradation when compared with the effect of multiple short rests, summing up the original rest time, distributed in each cycle. In all the previous cases, the effects due to the variation of the rest period were studied on the case in which the rest is introduced after a fixed amount of cycles or time, but not as distributed rests in each charge-discharge cycle.

The experiments presented in this work were performed to identify the effect of a rest time after a full charge in the battery performance degradation. Two batteries were cycled using constant current (CC)-constant-voltage (CV) profiles for both charge and discharge. Their rest periods between charge and discharge in each cycle are one hour and one minute. Hence, both a long and a short rest time are considered. During the experiment, the values of the current, the voltage, the SOC and the temperature of the batteries were acquired with a sampling time of one second. In order to evaluate the impact of the rest time, an analysis and a comparison of the variations in the battery capacity, charge-discharge times, voltage evolution during the rest period, and internal resistance were performed.

The paper is organised as follows. Section II describes the performed experiments, the test-bed and the charge-discharge profiles. Then, Section III reports on the data acquired during the cycling tests, and in Section IV discusses the results in terms of capacity, resistance and time variations with degradation for both batteries. Finally, Section V draws some conclusions.

II. EXPERIMENT DESCRIPTION

The LiFePO₄-based batteries used in this study are the Goodwolfe X-2E with a nominal capacity of 15 A h⁻¹. These batteries, mainly used in the electric vehicles sector, are shown in Fig. 1, while Tab. I lists their specifications.

The test was performed at room temperature using a battery pack test system NHR 9200, operating at The University of Manchester. The system includes six power modules for battery cycling. Two of those modules, each including a source and a sink of current up to 40 V and 600 A, have been used for the power conditioning of the two batteries under test. A typical CC-CV profile is used both for battery charge and discharge. The typical battery charge-discharge cycles are depicted in 2 for both batteries under test. The charge-discharge cycle starts by setting a current of 15 A, which is kept until the battery voltage reaches 3.64 V. This voltage is



Fig. 1. Picture of Goodwolfe X-2E batteries

TABLE I
GOODWOLFE X-2E BATTERIES SPECIFICATIONS

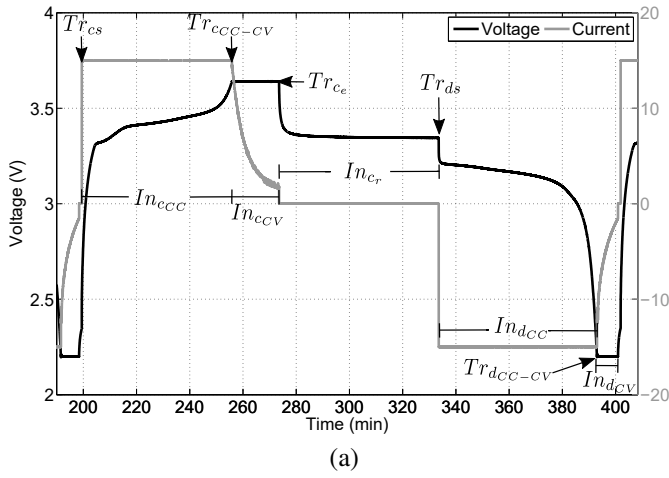
Nominal voltage	3.2 V
Capacity	15 A h
Maximal charge current	30 A (2C)
Maximal continuous discharge current	75 A (5C)
Maximal pulse discharge current	120 A (8C)
Overvoltage protection	3.65 V
Undervoltage protection	2.2 V
Impedance	< 5 mΩ
Discharge temperature	-20 °C / 60 °C
Life cycle	2000

kept constant until the charging current drops under 1.5 A, that is 10% of the CC current. At this point, the battery is considered to be fully charged and a rest period starts, while the voltage relaxes towards the steady-state open circuit voltage value. One of the batteries rests for one minute (short rest), while the other one rests for one hour (long rest). After the rest time, the battery is discharged at a constant current of -15 A, until the voltage reaches the lower threshold of 2.2 V. Then, the system switches to a constant-voltage discharge until the current goes below 1.5 A (absolute value). Once the battery has been fully discharged, a new CC-CV cycle starts after a rest of one minute for both batteries. With reference to the measurements, the accuracy values are 0.05% for the voltages, 0.1% for the currents, and 0.12% for the powers.

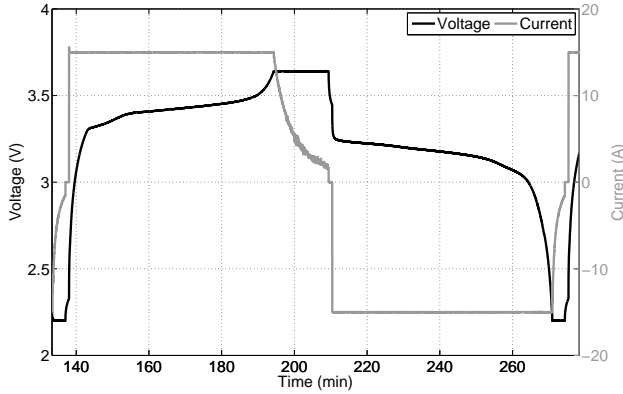
III. DATASETS DESCRIPTION

The data collected for each battery consists of samples taken every second, including the timestamps, the values of current, voltage, SOC, and room and cell temperatures.

Two examples of battery current and voltage during one single full cycle are presented in Fig. 2 for the two batteries. For reference purposes, the different sections in the cycle are labeled in Fig. 2(a). In this figure, the considered sections are six transitions, identified as $Tr_{x,y}$, and six intervals, identified as $In_{x,y}$. Here x indicates if the section is placed during charge, $x = c$, or discharge, $x = d$, and y is associated to the specific section: s for start, e for end, r for a rest interval, CC and CV for the constant current and constant voltage sections, and $CC - CV$ for the transition between a CC and a CV sections. It is worth mentioning that the transition corresponding to the end of discharge ($T_{d,e}$) and the rest after discharge interval



(a)



(b)

Fig. 2. Samples of the battery charge-discharge cycle. The battery is at rest after charge. (a) Battery-long, 1 h rest time after charge. (b) Battery-short, 1 min rest time after charge.

(In_{dr}) were also considered, but they were not shown in figure 2(a).

The charged (Q_c) and discharged (Q_d) capacity of the battery at any given time were computed making use of the Coulomb count method in the corresponding charge or discharge subcycles. The integral of the battery current, required by the Coulomb count, is approximated using the cumulative trapezoidal method. In a similar way, the charged (E_c) and discharged (E_d) energy were computed, by applying the cumulative trapezoidal method to the product of the battery voltage and current. Measurements of the time duration of the complete charge and discharge subcycles, and all the CC and CV phases were also taken. In each cycle equivalent ohmic resistances are computed at the beginning ($R_{s_{cs}}$) and at the end $R_{s_{ce}}$ of the charge and of the discharge, $R_{s_{ds}}$ for the start and $R_{s_{de}}$ for the end, as shown in Fig. 3. The individual resistance values are computed as the ratio of the variation between two consecutive samples of the voltage over the respective variation in the current. In this way, for example, $R_{s_{cs}}$ can be calculated as the difference of the voltages, ΔV_{cs} , over the difference of the currents, ΔI_{cs} , between the two samples belonging to Tr_{cs} in each cycle, as illustrated in Fig. 3.

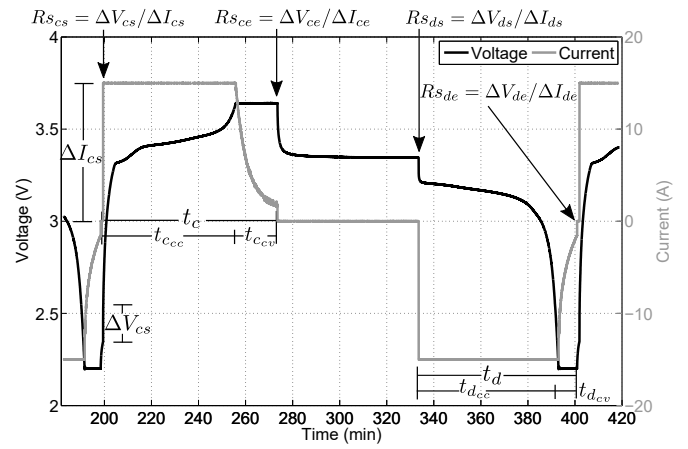


Fig. 3. Measured times and calculated resistances during one cycle

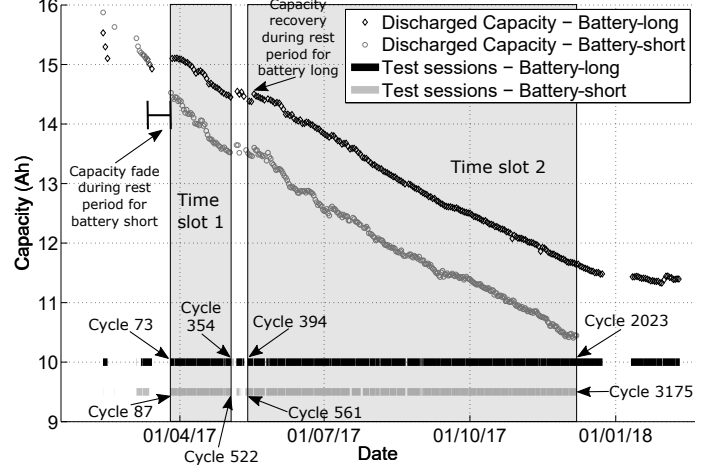


Fig. 4. Discharged capacity degradation against date and continuous test durations

The batteries were not cycled continuously during the whole experiment. The cycles were performed during sessions of various duration, which not necessarily coincide for both batteries as shown for the bars in the low part of Fig. 4.

Fig. 4 presents the capacity evolution of both batteries during the experiments. For the battery cycled with a rest of one hour between charge and discharge in each cycle, henceforth referred as Battery-long, 2426 full cycles distributed in 59 test sessions were acquired during the span of almost one year, reaching a capacity fade of 26.78%. In the other hand, for the battery with a rest of one minute between charge and discharge, namely Battery-short, the data includes 3175 complete charge-discharge cycles performed in 64 test sessions, ending with a reduction of capacity of 34.29%. It is worth mentioning that the capacity fade reached in the cycle number 2426 for Battery-short is 29.47%, presenting an higher overall total reduction in the capacity for the same amount of cycles than Battery-long. Nevertheless, this cannot be taken as an indicator of higher degradation for the battery with the shortest rest time, because the total capacity variations from the beginning of the experiment are not only affected by the

cycling, but also by the rest periods between test sessions.

The reduction of the battery capacities with time is evident for both cases, but it should be noted that the capacity variations not only occur during the periods of continuous cycling, as highlighted in Fig. 4. Indeed, between two consecutive sessions, the capacity might present a reduction, which most likely can be related to calendar aging, or an increment, which in general can be related to the capacity recovery phenomenon [10]. In order to exclude the effects of these intersession variations, two time slots including consecutive test sessions, separated the one another by less than 36 h, were used for both batteries. The first session goes from 25/03/2017 to 03/05/2017, and the second from 13/05/2017 to 07/12/2017. These ranges are highlighted in the figure.

IV. RESULTS

For a fixed time window, the battery with the shortest rest time was cycled more times. Considering this, for the two selected time slots, the variations of the parameters were analyzed for a limited amount of cycles counted since the start of the whole experiment. The selected sets of cycles correspond to those in which the count since the start of the experiment is the same for both batteries. As a result, two sets of cycles were identified: from cycle 100 to the cycle 354, and from the cycle 600 to the cycle 2023.

A. Capacity degradation

Fig. 5 presents the evolution of Q_d during the two selected cycle sets for both batteries. For the two batteries in the two analysed cycles sets, the capacity fade per cycle, ΔQ_d , was approximated as the negative of the slope of the linear fit to the data presented in Fig. 5. These fade rates are presented in Tab. II, which also includes the value of the coefficient of determination R^2 in each cases. The values of R^2 obtained for all the linear fits, over 94% in all cases, evidence the approximately linear degradation tendency of Q_d under the cycling experiment performed.

In both the analyzed sections, the battery cycled with the one hour rest time presents the highest value of ΔQ_d . Moreover, the differences between the two battery degradation rates are under 0.004%/cycle in both sections, and it is not possible to discern whether this is due to the inherent variability between the batteries or in the experiments. These results, obtained in the experiments introducing a rest period in each cycle, are in agreement with those obtained for experiments with rest periods included only after a fixed amount of cycles or time presented in the literature [5], [6], [11]. In these cases, it was established that a noticeable reduction in capacity fade, for an increasing rest time, is only observed when the rest time is in the ranges of several hours or days.

B. Energy efficiency

Similar tendencies were observed when considering E_d as a function of the cycle number, and for the energy efficiency $\eta = E_d/E_c$. These results are introduced in Fig. 6 in both cycling windows. For both batteries during each set of cycles

TABLE II
PERCENT Q_d FADE (%/CYCLE) FOR BOTH BATTERIES

Cycling window	Battery-long		Battery-short	
	ΔQ_d	R^2	ΔQ_d	R^2
1	0.0182	0.9845	0.0149	0.9471
2	0.0113	0.9915	0.0091	0.9838

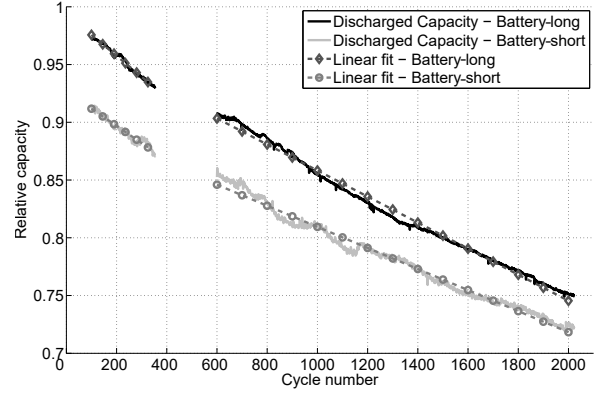


Fig. 5. Discharged capacity fade against cycle number during both cycling windows selected

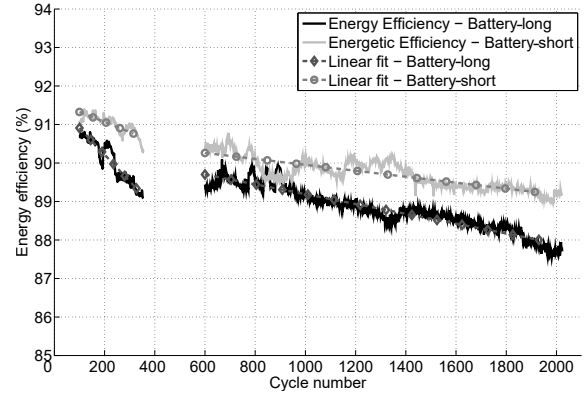


Fig. 6. Energy efficiency against complete cycle number during the two cycling number selected

considered, the energy efficiency η reduces in percentages under the 2%, which might be associated with the increase in the series resistance of the batteries with the aging. Again, a small difference in the variation rate between both batteries was found, under 0.5%/100 cycles in the two cycling windows.

C. Variations in the relaxation voltage evolution

The voltages at the end of the relaxation period after charge (V_{1h} – Battery-long and V_{1m} – Battery-short) were evaluated, and their variations with the cycle number are presented in Fig. 7. For the sake of comparison, this figure also introduces the voltage after one minute for the battery with the one hour rest period V_{1m} (Battery-long). As expected, the final open circuit voltage value after the longest relaxation period is the lowest one, as this value is closer to the actual open

circuit voltage at rest in full charge state. Additionally, the voltage after one-minute rest for Battery-long is always higher than the one for Battery-short in the studied cycling windows. This is also in accordance with the overall higher capacity values reported for Battery-long in figure 5. Finally, it is worth mentioning that in all cases the variations in the considered voltages with cycling are in the range of a few μV .

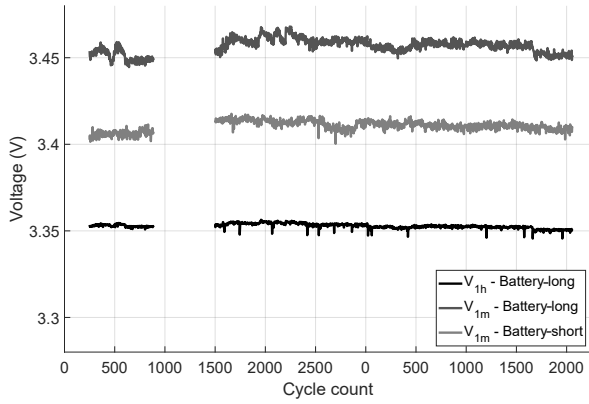


Fig. 7. Voltages at the end of the rest period for both batteries and voltage at one minute after the start of the rest for Battery-long during both studied cycling windows

The voltage transient during the relaxation interval was also evaluated at different cycle counts, as shown in Figs. 8 and 9. In both cases, it was not possible to identify any specific tendency that can be related with the aging of the batteries. The observed variation may be a consequence of the changes in the batteries impedance due to aging. The battery temperature may also deeply affect this parameter. A further investigation of the evolution of 3τ (three times the time constants of the voltage evolution, measured as the time taken to reach approximately the 95% of the overall voltage variation) for Battery-long, presented in Fig. 10, revealed no apparent degradation tendency.

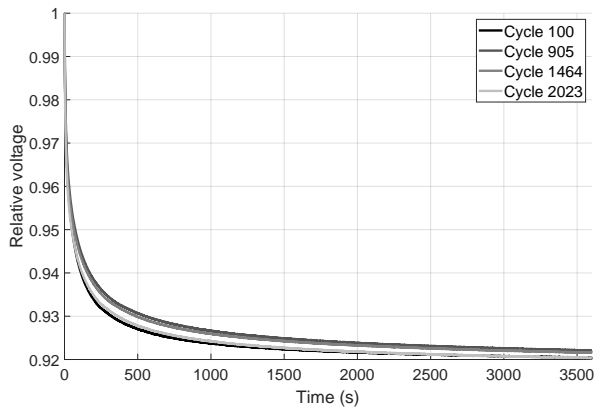


Fig. 8. Relative voltage evolution during rest after full charge at different degradation stages for the battery with the rest time of one hour

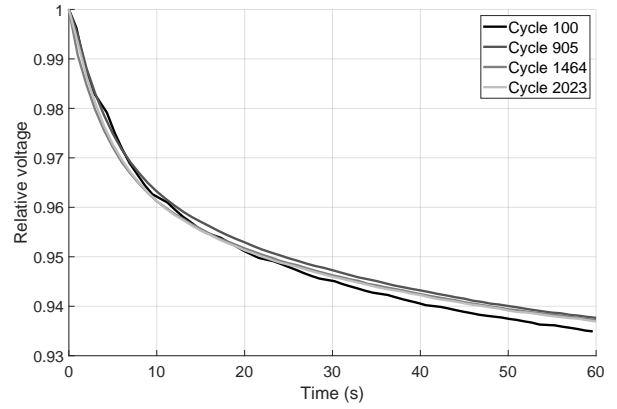


Fig. 9. Relative voltage evolution during rest after full charge at different degradation stages for the battery with the rest time of one minute

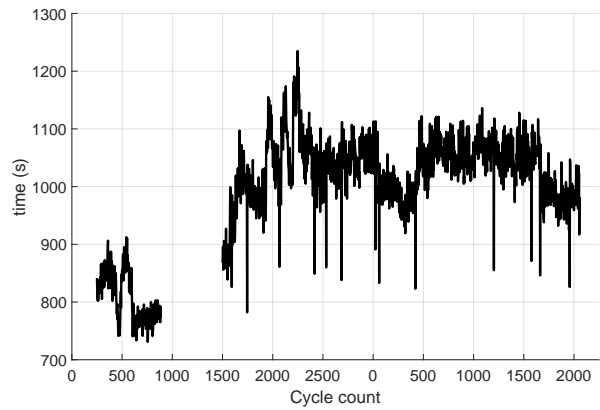


Fig. 10. Value of three times the time constant of the voltage during rest after full charge for the two interest cycling windows

D. CC time during discharge

The charge and discharge times, t_c and t_d respectively, and the CC times, $t_{c_{cc}}$ and $t_{d_{cc}}$ for charge and discharge, respectively, show an almost monotonic decreasing behavior. For example, the reductions of $t_{d_{cc}}$ as a function of the cycle number during both cycling windows are presented in Fig. 11. The $t_{d_{cc}}$ decreasing behavior with aging was expected. However, it is worth noting the similarity of the degradation tendencies for the CC times with the ones obtained for Q_d . The investigation of the relationships between these variables, which could be used for SOH estimation purposes, is worth to be matter of future work.

E. Equivalent series resistance

Due to the nature of the computation, the calculated series resistance values contain high noise values. For this reason, the analysis is performed after applying a moving average filter to the rough data. In general, all the resistances increases with the cycle number, as expected for aging batteries. The resistance values obtained are between 3.9 and 6 $\text{m}\Omega$ for Battery-long, and between 4.5 and 7.7 $\text{m}\Omega$ for Battery-short. In both cases

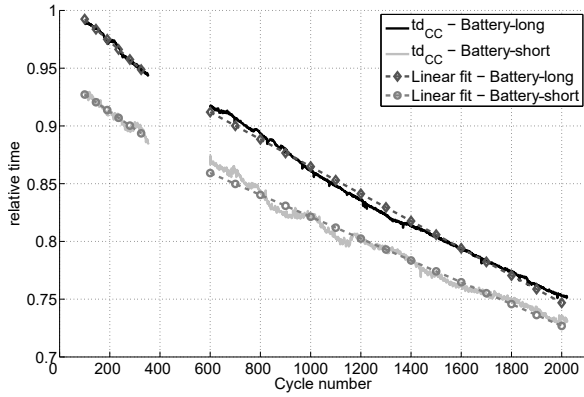


Fig. 11. Relative value of the time during the constant current part of the discharge against relative cycle number in the two cycling number selected

the initial values are inside the bound $< 5 \text{ m}\Omega$ presented in Tab. I and both final values are over the nominal maximum value after the experiment. The increase of $R_{s,ds}$ with cycling is presented in Fig. 12 for both cycling windows. In this case, a higher increase of $R_{s,ds}$ for Battery-long was observed in both cycling windows. This could be the cause of the lower energy efficiency observed for Battery-long in Fig. 6.

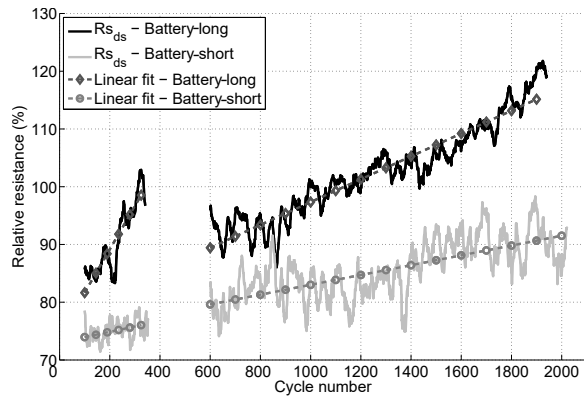


Fig. 12. Relative value of the resistance computed during discharge start filtered and corresponding linear fit during the two cycling windows selected

V. CONCLUSIONS

Two lithium-ion batteries were subjected to full charge-discharge cycling tests with different rest times after full charge. The changes due to the cycling degradation were compared in order to determine whether the variation in the rest time has any valuable effect.

Even if a overall higher capacity reduction was reached for the battery with the shortest rest time, the observed degradation rates during continuous cycling periods were generally higher for the battery with the longest rest period. Furthermore, this battery also presented a lower energy efficiency and a higher rate of internal resistance increase during the whole experiment. However, due to the relative small variations in

the degradation characteristics between the two batteries, it was concluded that they might be related to initial differences in the batteries and in the tests conditions, for instance the temperature. It is possible that, considering the comparison of rest times in each cycle of several hours or even days may reveal dependencies for the degradation dynamics that were not distinguishable for the orders of magnitude considered in this experiment. This result seem to be compatible with the available literature.

REFERENCES

- [1] M. Bruder Müller, B. Sobotka, and D. Waughray, "A Vision for a Sustainable Battery Value Chain in 2030 Unlocking the Full Potential to Power Sustainable Development and Climate Change Mitigation," World economic forum, Tech. Rep. September, 2019. [Online]. Available: http://www3.weforum.org/docs/WEF_A_Vision_for_a_Sustainable_Battery_Value_Chain_in_2030_Report.pdf
- [2] A. Eddahech, O. Briat, H. Henry, J. Y. Delétage, E. Woïgard, and J. M. Vinassa, "Ageing monitoring of lithium-ion cell during power cycling tests," *Microelectronics Reliability*, vol. 51, no. 9-11, pp. 1968–1971, 2011. [Online]. Available: <http://dx.doi.org/10.1016/j.microrel.2011.07.013>
- [3] A. Eddahech, O. Briat, E. Woïgard, and J. M. Vinassa, "Remaining useful life prediction of lithium batteries in calendar ageing for automotive applications," *Microelectronics Reliability*, vol. 52, no. 9-10, pp. 2438–2442, 2012. [Online]. Available: <http://dx.doi.org/10.1016/j.microrel.2012.06.085>
- [4] L. Lu, X. Han, J. Li, J. Hua, and M. Ouyang, "A review on the key issues for lithium-ion battery management in electric vehicles," *Journal of Power Sources*, vol. 226, pp. 272–288, 2013. [Online]. Available: <http://dx.doi.org/10.1016/j.jpowsour.2012.10.060>
- [5] B. Epping, B. Rumberg, H. Jahnke, I. Stradtman, and A. Kwade, "Investigation of significant capacity recovery effects due to long rest periods during high current cyclic aging tests in automotive lithium ion cells and their influence on lifetime," *Journal of Energy Storage*, vol. 22, no. February, pp. 249–256, 2019. [Online]. Available: <https://doi.org/10.1016/j.est.2019.02.015>
- [6] M. Reichert, D. Andre, A. Rösman, P. Janssen, H. G. Bremes, D. U. Sauer, S. Passerini, and M. Winter, "Influence of relaxation time on the lifetime of commercial lithium-ion cells," *Journal of Power Sources*, vol. 239, pp. 45–53, 2013. [Online]. Available: <http://dx.doi.org/10.1016/j.jpowsour.2013.03.053>
- [7] Z. Wang, S. Zeng, J. Guo, and T. Qin, "State of health estimation of lithium-ion batteries based on the constant voltage charging curve," *Energy*, vol. 167, pp. 661–669, 2019. [Online]. Available: <https://doi.org/10.1016/j.energy.2018.11.008>
- [8] I. Baghdadi, O. Briat, P. Gyan, and J. M. Vinassa, "State of health assessment for lithium batteries based on voltage–time relaxation measure," *Electrochimica Acta*, vol. 194, pp. 461–472, 2016. [Online]. Available: <http://dx.doi.org/10.1016/j.electacta.2016.02.109>
- [9] E. Schaltz, D. I. Stroe, K. Norregaard, B. Johnsen, and A. Christensen, "Partial charging method for lithium-ion battery state-of-health estimation," *2019 14th International Conference on Ecological Vehicles and Renewable Energies, EVER 2019*, pp. 4–8, 2019.
- [10] A. Eddahech, O. Briat, and J. M. Vinassa, "Lithium-ion battery performance improvement based on capacity recovery exploitation," *Electrochimica Acta*, vol. 114, pp. 750–757, 2013. [Online]. Available: <http://dx.doi.org/10.1016/j.electacta.2013.10.101>
- [11] S. Grolleau, I. Baghdadi, P. Gyan, M. Ben-Marzouk, and F. Duclaud, "Capacity fade of lithium-ion batteries upon mixed calendar / cycling aging protocol," in *International Battery, Hybrid and Fuel Cell Electric Vehicle Symposium*, Montréal, Canada, 2016. [Online]. Available: <https://hal.archives-ouvertes.fr/hal-01363521>
- [12] E. Cuervo-Reyes and R. Flückiger, "One law to rule them all: Stretched exponential master curve of capacity fade for Li-ion batteries," *Journal of the Electrochemical Society*, vol. 166, no. 8, pp. A1463–A1470, 2019.
- [13] L. Su, J. Zhang, C. Wang, Y. Zhang, Z. Li, Y. Song, T. Jin, and Z. Ma, "Identifying main factors of capacity fading in lithium ion cells using orthogonal design of experiments," *Applied Energy*, vol. 163, pp. 201–210, 2016. [Online]. Available: <http://dx.doi.org/10.1016/j.apenergy.2015.11.014>